

# Semianalytic approach for analyzing coupling issues in photonic crystal structures

P. Sanchis<sup>a)</sup> and J. Marti

Nanophotonics Technology Center, Universidad Politécnica de Valencia, Camino de Vera s/n, 46022, Valencia, Spain

P. Bienstman and R. Baets

Ghent University, Department of Information Technology, Interuniversity Micro-Electronics Centre (IMEC), Sint-Pietersnieuwstraat 41, B-9000 Gent, Belgium

(Received 22 February 2005; accepted 19 September 2005; published online 9 November 2005)

A semianalytic approach based on previously derived closed-form expressions for the transmission and reflection matrices between a dielectric waveguide and a semi-infinite photonic crystal (PhC) waveguide is proposed for analyzing coupling issues in PhC structures. The proposed approach is based on an eigenmode expansion technique and introduces several advantages with respect to other conventional numerical methods such as a shorter computation time and the possibility to calculate parameters, such as the reflection into PhC structures, difficult to obtain with others methods. Two different examples are analyzed and results compared to finite-difference time-domain simulations to prove the usefulness of the proposed approach: (i) An especially designed two-defects configuration placed within a PhC taper to improve the coupling efficiency and (ii) a coupled-cavity waveguide coupled to a single-line defect PhC waveguide. © 2005 American Institute of Physics. [DOI: 10.1063/1.2130528]

Photonic crystals (PhCs), periodic structures with a period of the order of the wavelength of light, have been the subject of an increasing research effort due to their ability for controlling the flow of light.<sup>1</sup> An efficient coupling into PhC structures is a crucial issue to ensure their optimum performance. In recent years, a large variety of different coupling techniques have been proposed and evaluated by means of simulation. However, the modeling of the interface between PhC structures and external media with efficient and accurate approaches may significantly reduce the computation time, which is usually very long in conventional numerical methods such as the finite-difference time-domain (FDTD) method.<sup>2</sup> Different kinds of approaches have been proposed in the last years based on the scattering matrix,<sup>3</sup> the expansion of the electromagnetic field into Wannier functions,<sup>4</sup> Fourier-modal methods,<sup>5</sup> the concept of impedance derived from the transmission line theory,<sup>6</sup> or Bloch mode expansion based methods.<sup>7-10</sup> In this letter, previously derived closed-form expressions based on an eigenmode expansion technique are proposed for analyzing coupling issues in more complex PhC structures by means of a semianalytic approach.

Let us consider the structure shown in Fig. 1. A dielectric waveguide is coupled to a semi-infinite PhC waveguide by using an especially designed two-defects configuration placed within a PhC taper. The proposed semianalytic approach is based on using the same transmission and reflection matrices derived in Refs. 11 and 12 and defined as

$$T = F_+^{-1}(I - R_{21}B_+F_+^{-1})^{-1}T_{12}, \tag{1}$$

$$R_{IN} = R_{12} + T_{21}B_+T, \tag{2}$$

$$R_{OUT} = -(B_- - R_{21}F_-)^{-1}(B_+ - R_{21}F_+), \tag{3}$$

where  $F_+$  ( $F_-$ ) and  $B_+$  ( $B_-$ ) are the forward and backward components of the forward (backward) Bloch modes that propagate in the PhC, medium II in Fig. 1, while  $T_{12}$ ,  $T_{21}$ ,  $R_{12}$ , and  $R_{21}$  are the transmission and reflection matrices for the structure placed between the dielectric and PhC waveguides, medium I-II in Fig. 1. For the structure shown in Fig. 1, the transmission,  $T$ , and reflection,  $R_{IN}$ , matrices describe the coupling for light propagating from the dielectric waveguide (medium I) into the PhC waveguide (medium II) while the reflection matrix,  $R_{OUT}$ , describes the coupling for light propagating from the PhC waveguide into the dielectric waveguide. The novelty with respect to our previous works reported in Refs. 11 and 12 is that  $T_{12}$ ,  $T_{21}$ ,  $R_{12}$ , and  $R_{21}$  must be calculated by using a numerical tool thus giving the semianalytic character to the proposed approach. In this

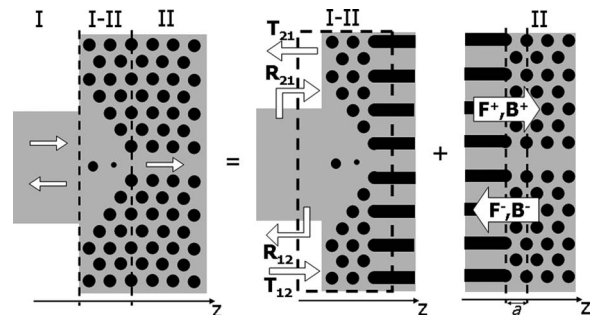


FIG. 1. Schematic of the proposed semianalytic approach for analyzing a structure formed by a dielectric waveguide coupled to a semi-infinite photonic crystal (PhC) waveguide by using an especially designed two-defects configuration placed within a PhC taper.  $T_{12}$ ,  $R_{21}$ ,  $T_{21}$ , and  $R_{12}$  are the transmission and reflection matrixes calculated in mediums I-II while  $F_+$  ( $F_-$ ) and  $B_+$  ( $B_-$ ) are the forward and backward components of the forward (backward) propagating Bloch modes calculated at the interface layer between mediums I-II and medium II, which corresponds to a fixed cut position within the lattice period,  $a$ , of the PhC. The  $z$  axis indicates the propagation direction.

<sup>a)</sup>Electronic mail: pabsanki@ntc.upv.es

case, a frequency-domain model based on a vectorial eigenmode expansion technique, known as CAMFR, has been used.<sup>13</sup> The forward and backward components of the Bloch modes are calculated at the interface layer between mediums I–II and medium II, which corresponds to a fixed cut position within the lattice period of the PhC, as depicted in Fig. 1. The forward propagating Bloch modes are distinguished from the backward propagating Bloch modes by looking at the power flux for the guided modes and at the imaginary part of the wave vector for the evanescent modes.

The structure shown in Fig. 1 have been first analyzed by considering a 3  $\mu\text{m}$ -wide dielectric waveguide of silica ( $n=1.45$ ) surrounded by an air cladding and a PhC formed by a two-dimensional triangular lattice of dielectric rods of silicon ( $n=3.45$ ) embedded in silica. The radius of the rods is  $R=0.2a$  where  $a$  is the lattice constant. This structure was previously analyzed by means of FDTD simulations in Ref. 14. It was shown that the transmission may significantly improve by properly setting a number of localized defects within the PhC taper. A two-defects configuration was designed following a heuristic approach based on firstly deciding the number and relative positions in the  $z$  axis of the defects placed within the PhC taper and then optimizing the radius of each defect. However, the proposed semianalytic approach allows a more accurate design by calculating all the possible solutions in terms of the radius and relative position of the defects. Figure 2(a) shows the transmission efficiency at the normalized frequency of  $0.3(a/\lambda)$  as a function of the defect radius normalized to the rod radius,  $r_{\text{def}}/R$ , and of the relative position in the  $z$  axis normalized to the lattice constant,  $z_{\text{def}}/a$ . It can be seen that there is a dominant maximum of 79% for a radius of  $r_{\text{def}}=1.03R$  and at a position of  $z_{\text{def}}=0.63a$ . This gives the true optimum position for a single defect. However, the transmission can be further improved by introducing an additional defect. The parameters of the defect are also designed by calculating the transmission map, which is shown in Fig. 2(b), but considering that the previous defect is located within the PhC taper. The transmission efficiency is improved up to 87% when the additional defect of a radius of  $r_{\text{def}}=0.34R$  is placed at  $z_{\text{def}}=1.63a$ . This efficiency is slightly higher than the one obtained in Ref. 14 as the parameters of the two-defects configuration are also somewhat different.

The previous analysis has been made possible because the computation time needed to calculate the maps shown in Fig. 2 is rather short by using the semianalytic method with respect to FDTD simulations. Notice that the total number of possible solutions is  $N=(2a/\Delta z) \cdot (2R/\Delta r)$ , where  $\Delta z$  and  $\Delta r$  are the steps related to the position and radius of the defect, respectively. Thus, for steps values of  $\Delta z=0.1a$  and  $\Delta r=0.1R$ , the total number of solutions is 400. Figure 3 shows the transmission spectra for the PhC taper with and without the optimized two-defects configuration. Semianalytic results are compared with FDTD simulations showing a very good agreement. Furthermore, it can be seen that the transmission is significantly improved when the two-defects configuration is placed within the PhC taper.

The proposed approach can also be used to analyze the transmission and reflection properties of more complex structures such as a coupled-cavity waveguide (CCW) coupled to a conventional single line defect PhC waveguide. The PhC parameters are the same as those previously used for the structure shown in Fig. 1. In this case, we are inter-

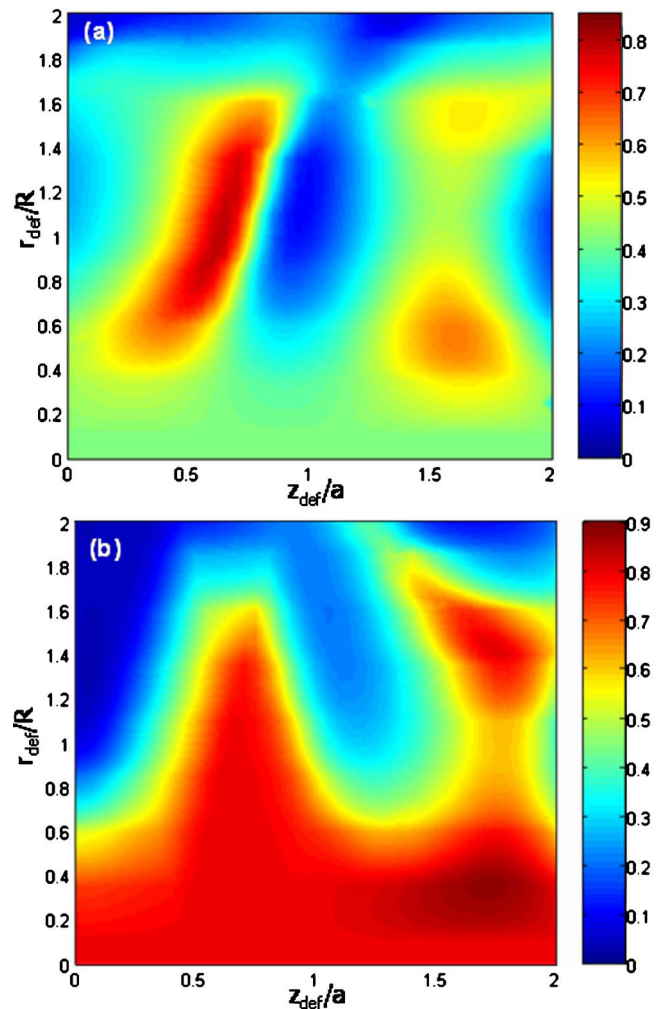


FIG. 2. (Color online) (a) Transmission efficiency as a function of the defect radius normalized to the rod radius of the photonic crystal,  $r_{\text{def}}/R$ , and of the relative position in the  $z$  axis within the PhC taper normalized to the lattice constant,  $z_{\text{def}}/a$ . (b) Transmission efficiency map of an additional single defect considering that a defect of radius  $r=1.03R$  is placed at  $z=0.63a$  within the PhC taper.

ested in calculating the reflection into the CCW when light propagates from the CCW into the PhC waveguide. In principle, both the CCW and the single line defect PhC waveguide are periodic so the proposed semianalytic approach

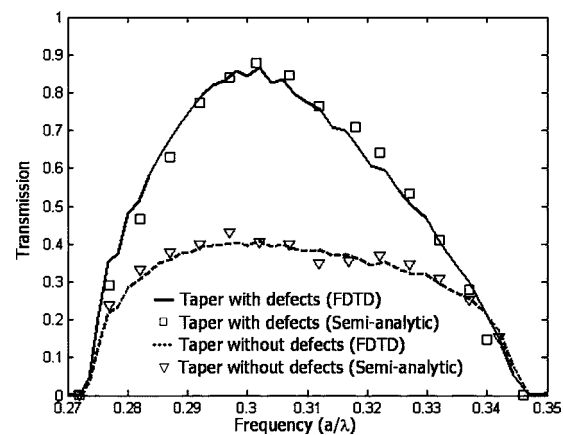


FIG. 3. Transmission efficiency as a function of the normalized frequency for the structure shown in Fig. 1 and considering the PhC taper with and without the optimized two-defects configuration. Semianalytic results are compared with FDTD simulations.

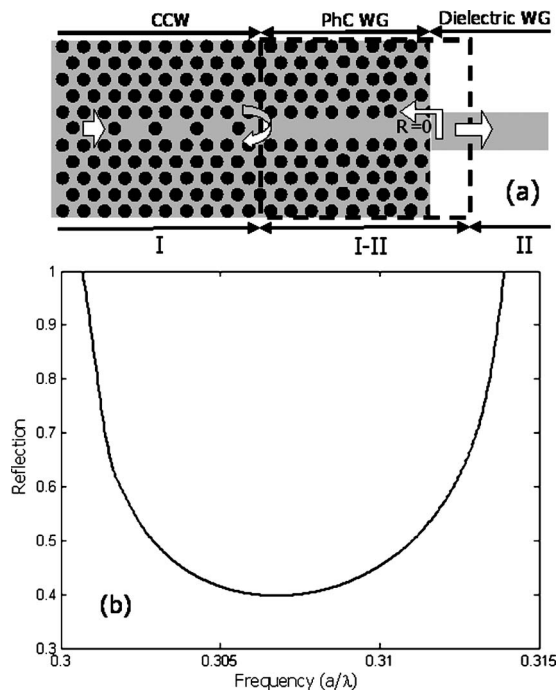


FIG. 4. (a) Coupled-cavity waveguide (CCW) coupled to a conventional single line defect PhC waveguide. The PhC waveguide is butt coupled to a  $0.5 \mu\text{m}$  wide dielectric waveguide by conveniently choosing the cut position to achieve negligible reflection back to the CCW. (b) Reflected power into the CCW as a function of the normalized frequency.

cannot be used. However, a simple trick can avoid this situation. Figure 4(a) shows the analyzed structure. The dashed square corresponds to mediums I-II in which  $R_{21}$  have to be numerically calculated by means of Eq. (3). The PhC waveguide has been butt coupled to a  $0.5 \mu\text{m}$  wide dielectric waveguide by conveniently choosing the cut position to achieve negligible reflection in the whole bandwidth of CCW.<sup>12</sup> This is possible because the bandwidth of the PhC waveguide is much broader than that of the CCW. Therefore, the reflection into the CCW, shown in Fig. 4(b), will only be the one that is originated due to inefficient coupling between the CCW and the single line defect PhC waveguide.

Reflection results can be used for efficiently modeling structures of finite length by means of the well-known Fabry-Perot formula. The propagation of ultra short pulses in CCWs of finite length was analyzed following this method.<sup>15</sup> The transmission response in amplitude of the Fabry-Perot (FP) formula can be written as

$$t_{\text{FP}}(f_n) = \frac{-t^2 \exp\left(-j\frac{2\pi}{a}kL\right)}{1 - r^2 \exp\left(-j\frac{4\pi}{a}kL\right)}, \quad (4)$$

where  $f_n$  is the normalized frequency,  $k$  is the normalized wave vector,  $L$  is the cavity length, and  $t$  and  $r$  are the transmission and reflection coefficients. The reflection coefficient is calculated as  $r = \sqrt{R}$ , where  $R$  is the reflected power shown in Fig. 4(b) and calculated by using the proposed semianalytic approach. On the other hand, the transmission coefficient is obtained as  $t = \sqrt{1-R}$  when single mode transmission and no radiation modes exist in the whole system.

Figure 5 shows the transmission spectrum calculated with (4) (dashed line) and by using the FDTD method (solid

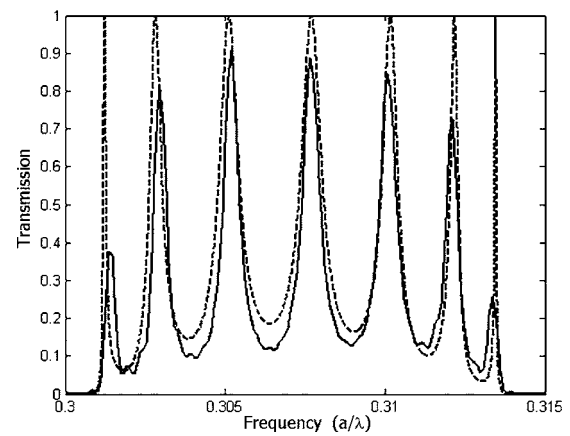


FIG. 5. Transmission spectrum of a CCW of finite length calculated by using the Fabry-Perot formula (dashed line) and by using the FDTD method (solid line).

line) for a seven cavity long CCW ( $L=16a$ ) coupled to the single line defect PhC waveguide. A very good agreement can be seen between the Fabry-Perot model and FDTD results. The amplitude of the resonance peaks, principally at the band edges, is lower in the FDTD simulation because a higher frequency resolution requires a very short time step, which would significantly increase the simulation time.

In summary, an efficient semianalytic approach has been proposed for analyzing coupling issues in PhC structures. The proposed approach is valid for any kind of complex structure as long as the input medium has an index profile invariant along the propagation direction and the output medium is semi-infinitely periodic along the propagation direction or vice versa.

This work has been partially funded by the Spanish Ministry of Science and Technology under Grant No. TIC2002-01553 and by the Generalitat Valenciana. P.S. acknowledges the Spanish Ministry of Education, Culture and Sport for funding his grant. This work has also been partially funded by the European Commission under the framework of the PHOLOGIC FP6 Project IST-NMP-2-017158.

<sup>1</sup>J. D. Joannopoulos, R. D. Meade, and J. N. Winn, *Photonic Crystals* (Princeton University Press, Princeton, NJ, 1995).

<sup>2</sup>A. Taflov, *Computational Electrodynamics: The Finite-Difference Time-Domain Method* (Artech House, Norwood, MA, 1995).

<sup>3</sup>S. F. Mingaleev and K. Busch, *Opt. Lett.* **28**, 619 (2003).

<sup>4</sup>K. Busch, S. F. Mingaleev, A. Garcia-Martin, M. Schillinger, and D. Hermann, *J. Phys.: Condens. Matter* **15**, R1233 (2003).

<sup>5</sup>P. Lalanne and E. Silberstein, *Opt. Lett.* **25**, 1092 (2000).

<sup>6</sup>J. Ushida, M. Tokushima, M. Shirane, A. Gomyo, and H. Yamada, *Phys. Rev. B* **68**, 155115 (2003).

<sup>7</sup>Z. Y. Li and K. M. Ho, *Phys. Rev. B* **68**, 155101 (2003).

<sup>8</sup>Z. Y. Li and K. M. Ho, *Phys. Rev. B* **68**, 245117 (2003).

<sup>9</sup>L. C. Botten, A. A. Asatryan, T. N. Langtry, T. P. White, C. M. de Sterke, and R. C. McPhedran, *Opt. Lett.* **28**, 854 (2003).

<sup>10</sup>L. C. Botten, T. P. White, A. A. Asatryan, T. N. Langtry, C. M. de Sterke, and R. C. McPhedran, *Phys. Rev. E* **70**, 056606 (2004).

<sup>11</sup>P. Sanchis, P. Bienstman, B. Luyssaert, R. Baets, and J. Martí, *IEEE J. Quantum Electron.* **40**, 550 (2004).

<sup>12</sup>P. Sanchis, J. Martí, B. Luyssaert, P. Dumon, P. Bienstman, and R. Baets, *Opt. Quantum Electron.* **37**, 133 (2005).

<sup>13</sup><http://camfr.sourceforge.net>

<sup>14</sup>P. Sanchis, J. Martí, J. Blasco, A. Martínez, and A. García, *Opt. Express* **10**, 1391 (2002).

<sup>15</sup>P. Sanchis, J. García, A. Martínez, and J. Martí, *J. Appl. Phys.* **97**, 013101 (2005).